JOURNAL OF MATERIALS SCIENCE 31 (1996) 3501–3506

Crack initiation in laminated metal–intermetallic composites

J. RAWERS
US Bureau of Mines, Albany Research Center, Albany, OR 97321, USA
K. PERRY
Lockheed Idaho Technologies Company, Idaho Falls, ID 83415-2218, USA

Several mechanisms have been proposed to describe crack initiation and propagation in ductile–brittle composites. This experimental study shows that the failure of metal–intermetallic (metal–aluminides) composites was initiated by cracking initiation in the intermetallic layers. For metal layers that allowed shear deformation, crack initiation in adjacent intermetallic layers resulted from shear bands propagating from a crack tip in the intermetallic layer through the metal layer and producing stress concentration points at the interfaces of adjacent intermetallic layers. For metal layers that did not support shear deformation, crack initiation in the intermetallic layers resulted from the continued build up of stresses within the intermetallic layers, resulting in a relatively uniform distribution of cracks within the individual intermetallic layers. Prior to failure, lateral constraints produce lateral cracks in the intermetallic layers. The final fracture features of both failure mechanisms were similar for both metal–intermetallic systems.

1. Introduction

Failure of ductile–brittle composites systems have been experimentally studied and several theories proposed to describe the failure characteristics [1–7]. Most of these studies predict or indicate that crack initiation occurs first in the brittle layer. The type of crack propagation depends, amongst other factors, on the interface strength and the material properties of the individual layers [1–7]. In this study the failure characteristics, in particular the crack initiation and propagation, of two different ductile–brittle (metal– intermetallic) laminar composites are characterized. The thickness of the starting metal layers in the two different composites were varied so that, after processing, in one composite thin, high-strength, low ductile metal layers were produced whilst in the second composite thicker, lower strength, ductile metal layers were produced.

Laminated metal–intermetallic composites have been produced by laying-up sheets of different metal foils and processing them into the composite structure by heating the layered structure to a temperature where the intermetallic self-propagating, high-temperature, synthesis (SHS) reaction was initiated at the metal interfaces [8–10]. After the SHS reaction was completed, pressure was applied to the composite to produce a firmly bonded laminated metal–intermetallic composite. Post tensile test examination showed that composite failure was accompanied with extensive crack initiation within the intermetallic layers and ductile fracture in the metal layers [10]. Prior to complete failure, although numerous cracks were generated along the entire length of the intermetallic layers, no debonding or delamination occurred at the metal–intermetallic interface. The final fracture features of several different composite compositions were very similar in appearance, suggesting that similar failure mechanisms might control the failure of all these metal–intermetallic composites. Results from the current study show that the generation of the intermetallic cracks and their distribution depend upon the composite composition, most notably the mechanical properties of the metal layer and the stress–strain constraints resulting from the layer thickness.

In this study, a crossed diffraction grating was bonded to the edge of the metal–intermetallic composites. Phase shifting Moire interferometry [11] was used during the tensile loading to qualitatively observe the crack initiation, crack propagation, and failure process in two different laminar composites. Shortly after the samples exceeded tensile yielding, the test was stopped. The gratings remained firmly bonded to the metal–intermetallic surface and the regions of permanent strain in the composite structures was used to determine the deformation. The use of attached gratings in examining the deformed-fractured regions provided: (1) qualitative information to characterize the strain features within the two different metal–intermetallic composites, (2) an *in-situ* observation of crack initiation mechanisms in the intermetallic layers, and (3) an understanding of the eventual failure mechanim of the composites.

2. Experimentation

Two metal–intermetallic laminar composites were produced by laying up nickel or titanium foils between

0022–2461

TABLE I Starting foil thickness and composite layer thickness and composition.

	Prior to SHS reaction		After SHS reaction	
Al–Ni composite	Al 0.50	Ni 0.025	Al 0.40	NiAl 0.10
Ti–Al composite	Al 0.125	Ti 0.25	Ti 0.20	$TiAl_3$ 0.20

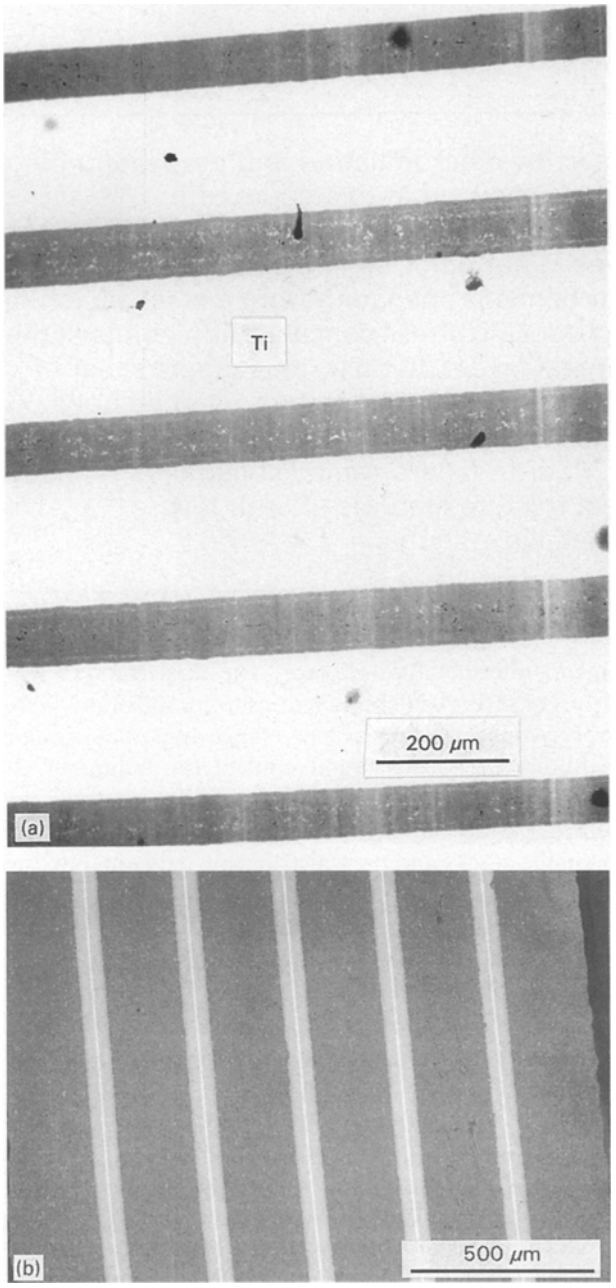

Figure 1 SEM micrograph of (a) the Ni–Ti and (b) the Ni–Al composites prior to testing.

alternating layers of aluminium foils (Table I). The foil sandwiches were then placed between graphite plates and heated to an appropriate bonding temperature. (For complete details on producing metal–intermetallic laminate composites using the SHS process see references 8–10.) The Ti–Al foil thickness was chosen so as to form a Ti–$TiAl_3$ composite, while the Ni–Al foil thickness was chosen so as to form an Al–NiAl

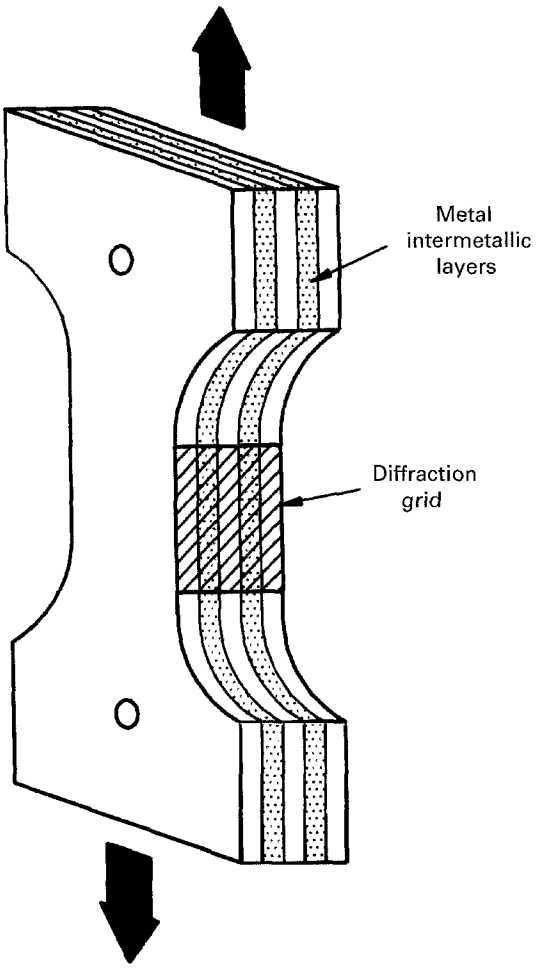

Figure 2 Schematic representation of the tensile sample and the replica grating.

composite. After the exothermic intermetallic reaction was completed, pressure was applied to ensure that a uniform and fully dense structure was produced. The final composite structure and composition are presented in Table I. The composite microstructure was examined and characterized by scanning electron microscopy (SEM) using back-scattering imaging and EDX stoichiometic analysis, typical microstructures are shown in Fig. 1.

Crossed, 300 lines mm^{-1} diffraction gratings were first bonded to the thin edge of the tensile samples (Fig. 2). The composite samples were then strained in tension. Phase shifting Moire interferometry was used to qualitatively observe the evolution of damage in the samples as the load was increased. Wrapped fringe patterns were recorded at various load levels. However, due to the high density of fringes, the images contained very little quantitative information. The use of lower frequency gratings (50 line mm^{-1}) will be used in future to overcome this difficulty.

The tensile test was monitored by a high-resolution charge coupled device (CCD) camera. The tensile strain rate was adjusted to monitor crack initiation and development of the failure mechanism. In order to evaluate only the initial stage of failure, i.e. crack initiation and propagation, the tensile tests were halted shortly after yielding (after approximately 5% strain). The plastic deformation in

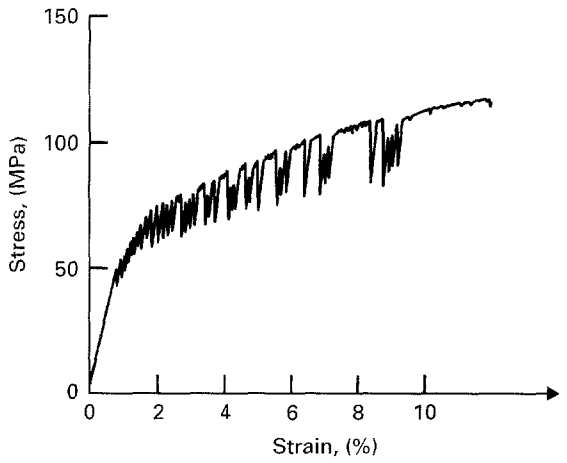

Figure 3 Stress–strain curve (Al–NiAl composite).

the individual layers was then determined qualitatively by examining the deformed spacing of the rulings under an optical microscope at 400× magnification. Plastic deformation was also examined using a scanning electron microscope.

A stress–strain curve for an Al–NiAl metal–intermetallic laminate composite is shown in Fig. 3. The serration in the fracture curves represent the initiation of cracks within the intermetallic layers. Optical and SEM examination of the surfaces show that prior to failure both composites had undergone extensive cracking within the individual intermetallic layers (Figs 4a and 5a).

3. Results and analysis

Observation of the diffraction gratings during and after the tensile tests showed that the two composites

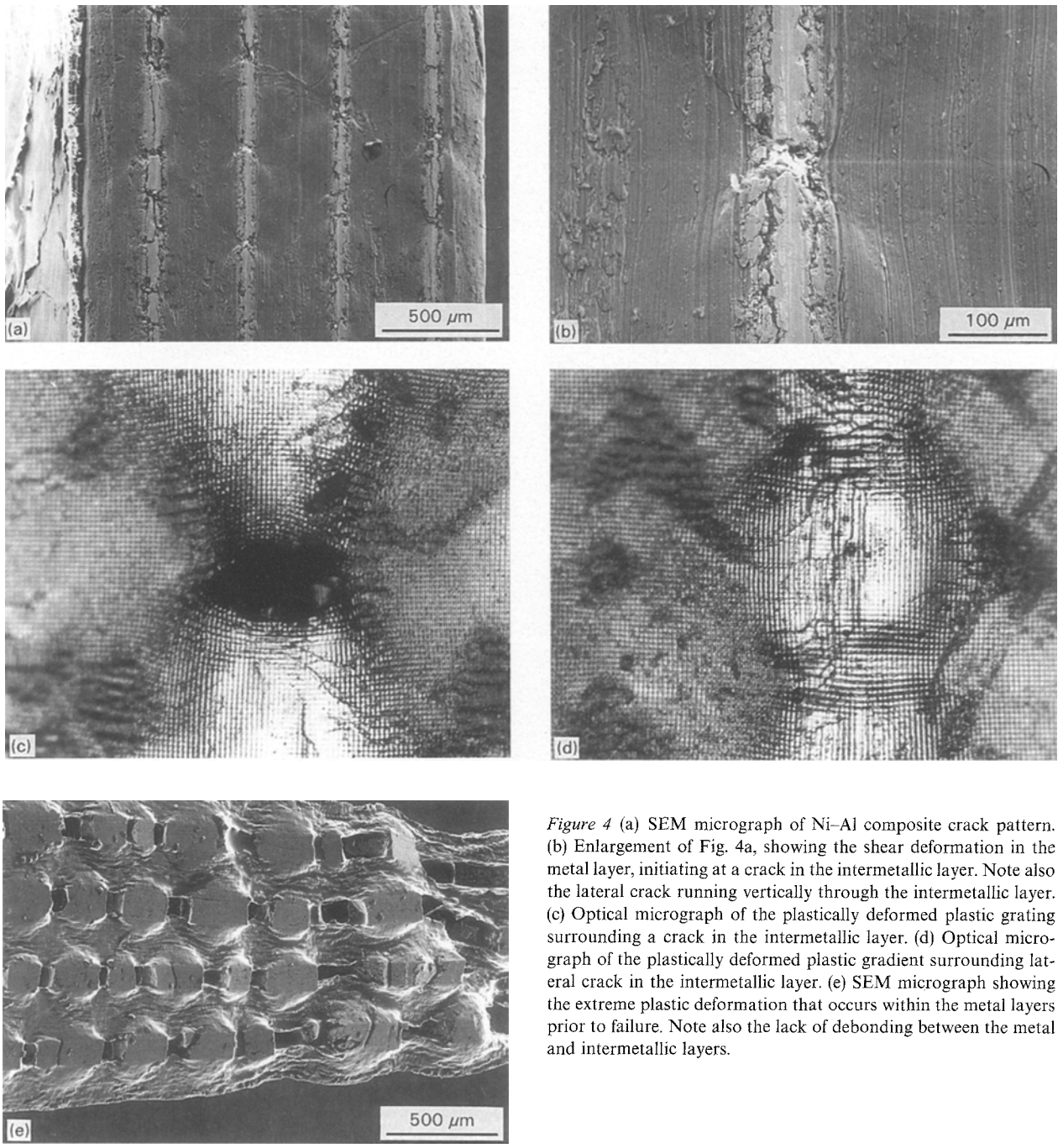

Figure 4 (a) SEM micrograph of Ni–Al composite crack pattern. (b) Enlargement of Fig. 4a, showing the shear deformation in the metal layer, initiating at a crack in the intermetallic layer. Note also the lateral crack running vertically through the intermetallic layer. (c) Optical micrograph of the plastically deformed plastic grating surrounding a crack in the intermetallic layer. (d) Optical micrograph of the plastically deformed plastic gradient surrounding lateral crack in the intermetallic layer. (e) SEM micrograph showing the extreme plastic deformation that occurs within the metal layers prior to failure. Note also the lack of debonding between the metal and intermetallic layers.

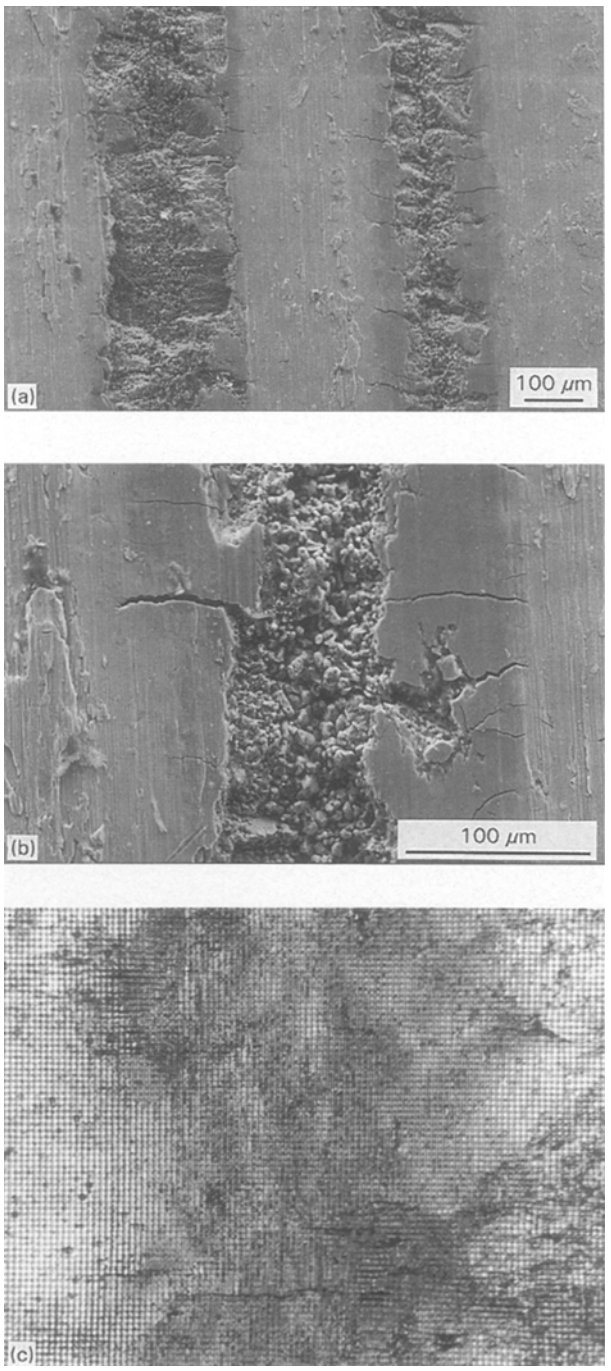

Figure 5 (a) SEM micrograph of Ti–Al composite rack pattern. (b) Enlargement of Fig. 4a, showing the cracking of the intermetallic phase. Note: the splitting of the cracks as they approach the metal interface. (c) Optical micrograph of the diffraction grating. Note in contrast to Fig. 4c the lack of plastic deformation in the grating surrounding the cracks in the intermetallic layer.

with different metal interface thickness responded differently to the applied stress. In both composites, cracks initiated in the intermetallic layer.

3.1. Al–NiAl composite

Crack initiation and generation in the Al–NiAl metal–intermetallic composite began with the initiation of a few, widely spaced cracks (Fig. 4a). These cleavage cracks extended across the entire width of the intermetallic layer and were terminated when they reached the adjacent metal layer interfaces. As the stress was increased, these cracks underwent crack-extension-opening or crack opening displacement (COD). The crack tip did not extend further into the metal layer but the crack tip radius increased and shear strains were observed to develop at the blunted crack tips. With increasing stress, the shear strain continued to develop and eventually extended completely across the metal layer, at approximately a 45° angle to the applied stress.

The plastic deformation associated with the terminated shear bands did not propagate into the less ductile intermetallic layer. Thus, when these shear bands reached the adjacent intermetallic layer, a stress concentration point developed. The metal–intermetallic interface bonding was sufficiently strong so that even in the presence of the stress concentration at the interface, no delamination was ever observed. Instead, the stress level increased in intensity until the combination of the applied tensile stress in the intermetallic layer and the stress concentration at the interface was sufficient to initiate a crack in the adjacent intermetallic layer. Thus, the initial crack acted as an initiation point from which a repeated series or cascade of cracks was generated.

With increasing strain, a series of shear–strain induced cracks was propagated into adjacent intermetallic layers. Eventually, the metal layers were saturated with the criss–cross shear–strain patterns (Fig. 4a) and further crack initiation was impossible. Further strain resulted in increased crack opening displacement and plastic deformation within the metal layer. Fig. 4(b, c) shows that at the crack tip the adjacent metal had undergone significant plastic deformation and a significant lateral contraction.

Examination of the diffraction gratings after extensive plastic deformation showed that the aluminium layer had developed a considerable amount of lateral stress. Lateral contraction in the metal layer introduced lateral stress on the intermetallic layers resulting in lateral cracks developing within the intermetallic layers. Prior to the final composite failure, these cracks rapidly extended down the length of the intermetallic layer (Fig. 4b and d). An example of extreme deformation within the metal layer is shown in Fig. 4e.

3.2. Ti–$TiAl_3$ composite

Crack initiation and development in the Ti–$TiAl_3$ metal–intermetallic composite was different from the Al–NiAl composite. Cracks were again initiated and were restricted to the intermetallic layers. However, with increasing strain, the intermetallic layers continued to develop random cracks throughout the intermetallic layers (Fig. 5a). There was no sign of shear bands developing within the metal layers. Cracking in the intermetallic layer was not controlled by the development of localized shear stress concentration points induced by the metal layer, but by the distribution of local defects in the intermetallic layer and the applied tensile stress (and stress redistribution resulting from cracking within the intermetallic layer). The crack distribution was not random but had a

statistical distribution of approximately 100 micrometers (Fig. 5(a–c)) which is approximately half the thickness of either the metal or intermetallic layer.

After extensive cracking across the intermetallic layers, cracks similar to the lateral cracks that formed in the Al–NiAl composite, formed in the Ti–$TiAl_3$ composites parallel to the stress direction and ran down the length of the outer intermetallic layers via the considerable number of lateral cracks previously described. This crack was again thought to have resulted from lateral stresses in the adjacent metal layers, i.e. from the difference in the stress levels in the metal layers at the free (outer) surface and the highly constrained metal layers in the interior of the composite.

4. Discussion

The difference in crack development between the Ti and $TiAl_3$ composite is thought to result from the difference in both the material characteristics of the metal layer and the strain characteristics that formed in the composite layers. Aluminium is a fcc phase metal, extremely ductile, and readily deforms by shear deformation. Titanium has a hcp-crystal structure and does not readily allow extensive plastic (shear) deformation. Therefore, unlike the fcc-aluminium layer, very limited shear strain was transferred through the titanium layer. The strain pattern in the titanium and the intermetallic layers was uniform. Thus, unlike the Al–NiAl composite, cracks in the Ti–$TiAl_3$ composite were continuously being initiated with increasing strain. No shear strain was observed generating from the crack tips in the titanium layer. Instead the plastic deformation after yielding was created by a small number of cracks opening and uniform plastic deformation in the metal and intermetallic layers. The difference in thickness of the metal layers in the two different composites may have resulted in control of the metal deformation. The thin titanium layer constrained the plastic deformation, whereas the thicker aluminium layer permitted plastic deformation.

Crack initiation and multiplication for the Al–NiAl and Ti–$TiAl_3$ metal–intermetallic composites resulted in a similar fracture appearance. However, the initial fracture sequence for the two composites was different (see Fig. 6). Fracture analysis showed that for both composite compositions, failure started by crack formation in the intermetallic layers. For the metal–intermetallic thickness ratios used in this study, the crack release energy of the intermetallic cracks was insufficient to propagate either the crack through the adjacent metal layers or to transfer sufficient energy through the metal layer to initiate cracks in the adjoining intermetallic layer. In the fcc-aluminium composite, the metal layer had sufficient plasticity to blunt the crack tip. The extensive deformation possible in the aluminium layer resulted in shear bands being generated from the crack tips thus producing stress concentration points and eventually crack initiation points in adjacent intermetallic layers. In the hcp-titanium composite, the intermetallic cracks were again terminated when they reached the metal interface. However, the limited ductility of the titanium limited the shear strain in the titanium layer. As a result, the generation of cracks in the intermetallic layer was controlled by the local defect structure of the intermetallics and the localized tensile stress of the composite structure.

In both metal–intermetallic composites, the interface bonding was sufficient to prevent delamination. Prior to failure, Poisson's stresses and shear stresses became sufficient to eventually produce lateral cracks within the intermetallic layers.

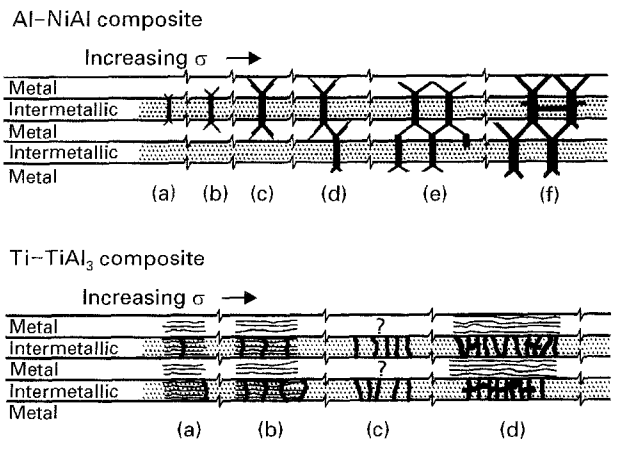

Figure 6 Schematic of crack initiation and multiplication sequence in the Ni–Al and Ti–Al metal intermetallic composites.

5. Summary

The results of this study indicate that the failure mechanism of metal–intermetallic composites depends upon the composite composition: more explicitly, upon the metal layer. Initially cracks that form in the intermetallic layer are terminated in the metal layer. The continued development of cracks by the intermetallic layer however depend upon the ductility (and possible metal layer thickness) of the metal layers. For highly ductile metals, such as aluminium, the crack multiplication mechanism is through development of stress concentrations resulting from plastic shear bands. For metals with limited ductility, such as titanium, the crack multiplication mechanism is a function of the global and local stress level and the distribution of defects within the intermetallic layer.

Current research is being directed to determine if the failure mechanism can be varied by controlling the metal to intermetallic thickness ratio for different metal layers.

References

1. M. F. ASHBY, F. L. BLUNT and M. BANNISTER, *Acta Matall. Mater.* **37** (1989) 1847.
2. H. E. DEVE, A. G. EVANS, G. R. ODETTE, R. MEHRABIAN, M. L. EMILLIANI and R. J. HECHT, *Acta Metall.* **38** (1990) 1491.
3. H. E. DEVE and M. J. MALLONEY, *ibid.* **39** (1991) 2275.
4. L. SIGL, P. A. MATAGA, B. J. DALGLEISH, R. M. McMEEKING and A. G. EVANS, *Acta Metall. Mater.* **36** (1988) 945.

5. M. F. BANNISTER and M. F. ASHBY, *Acta. Metall.* **39** (1991) 2575.
6. H. C. CAO and A. G. EVANS, *ibid.* **39** (1991) 2997.
7. M. C. SHAW, D. B. MARSCHALL, M. S. DADKHAH and A. G. EVANS, *ibid.* **41** (1993) 3311.
8. J. C. RAWERS, J. S. HANSEN, D. E. ALMAN and J. A. HAWK, *J. Mater. Sci. Lett.* **13** (1994) 1357.
9. D. E. ALMAN, J. A. HAWK, A. V. PETTY Jr. and J. C. RAWERS, *JOM* **46** (1994) 31.
10. D. E. ALMAN, J. C. RAWERS and J. A. HAWK, *Met. Trans. A* **26A** (1995) 589.
11. K. E. PERRY Jr., Optics and Lasers in Engineering (In press).

Received 25 April 1995
and accepted 1 December 1995